Prediction of CO Concentration and Maximum Smoke Temperature beneath Ceiling in Tunnel Fire with Different Aspect Ratio

S. Gannouni[†] and R. Ben Maad

Faculty of Sciences of Tunis, Department of Physics, Laboratory of Energizing and Thermal and Mass Transfer, 2092 ElManar, Tunis, Tunisia

†*Corresponding Author Email: gannounisoufien@gmail.com*

ABSTRACT

In a tunnel fire, the production of smoke and toxic gases remains the principal prejudicial factors to users. The heat is not considered as a major direct danger to users since temperatures up to man level do not reach tenable situations that after a relatively long time except near the fire source. However, the temperatures under ceiling can exceed the thresholds conditions and can thus cause structural collapse of infrastructure. This paper presents a numerical analysis of smoke hazard in tunnel fires with different aspect ratio by large eddy simulation. Results show that the CO concentration increases as the aspect ratio decreases and decreases with the longitudinal ventilation velocity. CFD predicted maximum smoke temperatures are compared to the calculated values using the model of Li *et al*. and then compared with those given by the empirical equation proposed by kurioka *et al*. A reasonable good agreement has been obtained. The backlayering length decreases as the ventilation velocity increases and this decrease fell into good exponential decay. The dimensionless interface height and the region of bad visibility increases with the aspect ratio of the tunnel cross-sectional geometry.

NOMENCLATURE

A_r	aspect ratio of tunnel cross-section	Q_c	convective heat release rate from fire
C_p	specific heat capacity	Q^*	dimensionless heat release rate
C_s	smagorinsky constant	Pr_t	Turbulent Prandtl number
D	diffusivity coefficient	r	radius of fire source
D^*	characteristic fire diameter	R	universal gas constant
f	external force vector	Sc_t	Turbulent Schmidt number
Fr	Froude number	T_a	ambient temperature
g	gravitational acceleration	t	time
h	specific enthalpy	**u**	velocity vector
h_{in}	interface height	V	ventilation velocity
h_{in}^*	dimensionless Interface height	$\overline{W}$	average molecular weight
h_l	enthalpy of lth species per unit mass	Y_l	mass fraction of lth species
H	runnel height	Z	mixture fraction
H_{ef}	height from the surface of fire source to tunnel ceiling	Δ	filter width in LES
k	thermal conductivity	ΔT_{max}	maximum excess smoke temperature
k_t	turbulent thermal conductivity	δt	time step
$\dot{m}_l'''$	production rate of lth species per unit volume	δx_i	grid size in direction
		μ_t	turbulent viscosity
p	pressure	ρ	density
$\dot{q}'''$	heat release rate per unit volume	ρ_0	ambient density
q_r	radiative heat flux vector	τ	stress tensor
Q	heat release rate from fire		

1. INTRODUCTION

The tunnel construction requires a long and an expensive works. Responsible are confronted permanently to the question of the structures stability of these underground infrastructures during their designs but also to the question of the people security and public confidence in the tunnels as sure means of transport. Indeed, the mine tunnels can be the seat of the economic life of entire regions. The road and railway tunnels participate to the improvement of transport networks and the preservation of the environment in urban areas. Among the potential dangers, the fires were identified among the dangerous phenomena and the most dreaded in the underground infrastructure. They arouse a particular concern because their consequences can be harmful if the adapted precautions do not request.

Numerous studies and investigations are focused on the analysis of the smoke dynamics and the physical phenomena involved in the tunnel fire situation. The studies of tunnel fires can be produced using various techniques. The full-scale testing, such as the tunnel Repparfjord tests (1990-1992) (PIARC, 1999) and the Memorial Tunnel experiments (1993-1995) (Massachusetts Highway Department and Bechtel/Parsons Brinckerhoff 1995), provide a database and important information on the smoke flow behavior but require expensive costs and means significant investigations and are limited in disused tunnels. The experimental scale models, in which they exist two types: cold and hot models, represent an interesting alternative to the full-scale tests and allow to make many necessary measures difficult to perform them in the full-scale experiments. However, the similarity cannot be completely reproduced for all parameters. A technique that has been known and which still knows important development is the CFD numerical modeling. This technique, which is based on numerical models, is more advantageous than the experimental methods in many points such as: wealth quantitative results, low cost and reduced time. However, the reliability of such numerical model and the data validity remain questionable until today, due to difficulties in modeling turbulence, combustion processes, etc.

The diverse methods of investigation of the tunnel fire problems and the research wealth are conducted to better understand the fire behavior as well is to improve the existing systems of safety. Indeed, the fire safety in the underground infrastructure to public use is become, at the same time, an important human and political issue. More than 80% of deaths during a fire are in relationship to the toxicity and the opacity of smoke. Hu *et al*. (2008) noted that the smoke particles and toxic gases released, such as carbon monoxide, are the most fatal contaminations and remain the prejudicial factors to users. Wang (2009) noted that the backlayering flow against the ventilation airflow carries the CO and soot production towards the tunnel entry. Hu *et al*. (2007) showed that the carbon monoxide concentration increases linearly with the height above the floor and

decreases exponentially with the distance away from the fire source. Zhang *et al*. (2012) found that the CO concentration is negatively correlated with the inclination angle and the thickness of the smoke layer and the smoke outflow rate are both positively correlated with the tunnel slope.

Moreover, the issue of fire safety is closely related to the foundation stability. The elevation of the smoke flow temperature under the ceiling is a source of degradation of the tunnel structure. In extreme cases, one can observe a collapse of the structure and this can create problems for emergency interventions. Several researches have focused on the study of the distribution of the maximum temperature of the smoke flow under the ceiling for fires in tunnels and corridors. Kurioka *et al*. (2003) suggests the following equation based on their experimental results in reduced scale:

$$\frac{\Delta T_{max}}{T_a} = \gamma \left(\frac{Q^{*2/3}}{Fr^{1/3}} \right)^{\varepsilon} \qquad (1)$$

$$Q^{*2/3}/Fr^{1/3} < 1.35, \; \gamma = 1.77, \varepsilon = 6/5$$

$$Q^{*2/3}/Fr^{1/3} \geq 1.35, \; \gamma = 2.54, \varepsilon = 0$$

With

$$Q^* = \frac{Q}{\rho_0 C_p T_a g^{1/2} H_{ef}^{5/2}} \qquad (2)$$

Fr is the Froude number

$$Fr = \frac{V^2}{gH_{ef}} \qquad (3)$$

Where Q is the heat release rate of fire and H_{ef} is the height from the surface of fire source to tunnel ceiling.

Recently, by performing experimental and theoretical studies, Li *et al*. (2011) have proposed the following model to predict the maximum excess gas temperature under the tunnel ceiling:

$$\Delta T_{max} = \begin{cases} \dfrac{Q}{V r^{1/3} H_{ef}^{5/3}}, & V' > 0.19 \\[2ex] 17.5 \dfrac{Q^{2/3}}{H_{ef}^{5/3}}, & V' \leq 0.19 \end{cases} \qquad (4)$$

With

$$V' = \frac{V}{V^*} \qquad (5)$$

$$V^* = \left(\frac{Q_c g}{r \rho_0 C_p T_a} \right)^{1/3} \qquad (6)$$

With Q_c and r is the convective heat release rate and the radius of fire source, respectively.

The present study seeks to analyze the smoke hazard such as the CO production as well the maximum smoke temperature under the ceiling in tunnel fire with different aspect ratio. Three-dimensional numerical simulations of large eddy of a fire in tunnel model are performed using an internationally recognized CFD code of the fire simulation (FDS). The CFD results are presented and analyzed.

2. NUMERICAL SIMULATION

The NIST fire dynamic simulator FDS is used in this study to perform the physical model configuration. FDS is a CFD open source software freely available for public from the NIST web site (www.fire.nist.gov/fds). This tool is built on a good approximation of Navier-Stokes equations appropriate to low Mach number applications. These equations are the equations of mass, momentum, energy and chemical species for a Newtonian fluid with the low Mach number assumption. These equations used in this study are given here (McGrattan *et al*. 2010a):

Mass equations

$$\frac{\partial \rho}{\partial t} + \nabla \cdot (\rho \mathbf{u}) = 0 \tag{7}$$

Momentum equations

$$\rho \left(\frac{\partial \mathbf{u}}{\partial t} + (\mathbf{u} \cdot \nabla) \mathbf{u} \right) + \nabla p = \rho g + \mathbf{f} + \nabla \cdot \tau \tag{8}$$

Energy equations

$$\frac{\partial (\rho h)}{\partial t} + \nabla \cdot \rho h \mathbf{u} - \frac{Dp}{Dt} = \dot{q}''' - \nabla \cdot q_r + \nabla \cdot k \nabla T + \nabla \cdot \sum_l h_l (\rho D)_l \nabla Y_l \tag{9}$$

Species equations

$$\frac{\partial (\rho Y_l)}{\partial t} + \nabla \cdot \rho Y_l \mathbf{u} = \nabla \cdot (\rho D)_l \nabla Y_l + \dot{m}_l''' \tag{10}$$

Equation of state

$$p = \frac{\rho R T}{\overline{W}} \tag{11}$$

The use of FDS is limited to low-speed flow. This approximation is largely sufficient for a fire-induced flow as the air velocity is lower than 10m/s and the ventilation velocity is less than 2m/s (Gao *et al*., 2004).

Turbulence models used in FDS are based on the large eddy simulation (LES) model and the direct numerical simulation (DNS) model. The LES model is retained in this study. LES model consists to separately treating the large- and the small-scale eddies by filtering. Filtering is operated by applying a low-pass filter, parameterized by a width *Δ*, of the equations system governing the flow. The subgrid model formulated in LES is established originally by Smagorinsky. The subgrid turbulent viscosity is modeled by (McGrattan *et al*. 2010a):

$$\mu_{ijk} = \rho (C_s \Delta)^2 \left(\begin{array}{l} 2\left(\frac{\partial u}{\partial x}\right)^2 + 2\left(\frac{\partial v}{\partial y}\right)^2 + 2\left(\frac{\partial w}{\partial z}\right)^2 \\ + \left(\frac{\partial v}{\partial x} + \frac{\partial u}{\partial y}\right)^2 + \left(\frac{\partial w}{\partial y} + \frac{\partial v}{\partial z}\right)^2 \\ + \left(\frac{\partial u}{\partial z} + \frac{\partial w}{\partial x}\right)^2 - \frac{2}{3}(\nabla . \mathbf{u})^2 \end{array} \right) \tag{12}$$

With C_s is the Smagorinsky constant.

The filter *Δ* is given by the following expression:

$$\Delta = V_m^{\frac{1}{3}} \tag{13}$$

Where V_m is the mesh volume. It is given by (McGrattan *et al*. 2010a):

$$V_m = \prod_{i=1}^{3} \delta x_i = \delta x \ \delta y \ \delta z \tag{14}$$

With $\delta x, \ \delta y, \ \delta z$ represent respectively the grid size in the three spatial directions.

Because of its sensitivity, the constant C_s is an important parameter. Although its theoretical value is worth 0.17 (Wen *et al*. 2007), much researchers propose other values for cases of applications quite specific extending from 0.1 to 0.25. For tunnel fire, it was reported that taking 0.2 for the Smagorinsky
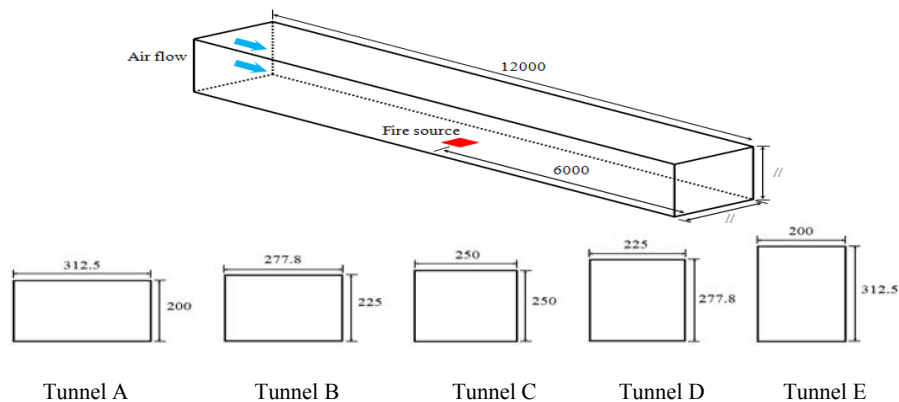
Fig. 1. Schematic of the tunnel model and the cross-sections (unit: mm).

constant is considered to be most appropriate, as the fire region is the driving force for the changes in the forced flow conditions within the tunnel (Kim *et al.* 2008).

The other diffusive parameters, the thermal conductivity and material diffusivity, are related to the subgrid turbulent viscosity by (McGrattan *et al.*, 2010a):

$$k_t = \frac{\mu_t Cp}{Pr_t} \tag{15}$$

$$(\rho D)_{l,t} = \frac{\mu_t}{Sc_t} \tag{16}$$

Where Pr_t is the turbulent Prandtl number and Sc_t is the turbulent Schmidt number. An effort of validation and checking was made for FDS. According to these validation works, the values 0.2, 0.5 and 0.5 are implanted by default in FDS for the constants C_s, Pr_t and Sc_t, respectively. Zhang *et al.* (2002) has tested tried different combinations of the Smagorinsky parameters, and suggested the current default values.

In FDS, the modeling of combustion is based on the mixture fraction concept for large-eddy simulation. The mixture fraction is a function of space and time, usually denoted $Z(x, t)$ and it satisfies the following conservation equation (McGrattan *et al.* 2010a):

$$\rho \frac{DZ}{Dt} = \nabla . \rho D \Delta Z \tag{17}$$

In a Single-Step Reaction, FDS5 considers a division of Z into the two following components:

$$Z_1 = \frac{Y_F}{Y_F^I} \tag{18}$$

$$Z_2 = \frac{W_F}{[x - \nu_{CO} - (1 - X_H)\nu_s] W_{CO_2}} \frac{Y_{CO_2}}{Y_F^I} \tag{19}$$

Such that Z is the amount of Z_1 and Z_2, $Z = Z_1 + Z_2$, Y_F^I is the mass fraction of fuel in the fuel stream, W_F is the molecular weight of the fuel, Y_{CO_2} is the mass fraction of CO_2, W_{CO_2} is the molecular weight of CO_2, $x - \nu_{CO} - (1 - X_H)\nu_s$ is the stoichiometric coefficient of CO_2, ν_{CO} is the stoichiometric coefficient of CO, ν_s represents the amount of fuel that is converted to soot, X_H is the hydrogen atomic fraction. The fraction of fuel mass converted into carbon monoxide, Y_{CO}, is linked to the soot yield, Y_s, via the correlation developed by par Koylu and Faeth (1991). The combustion model is coupled with a radiation model which determines thermal radiation transfer via the solution of the radiation transport equation (RTE) for a gray gas. RTE is solved using a technique similar to a finite volume method for convective transport.

To justify the stability of numerical scheme and to estimate the convergence calculation, the courant-Friedrichs-Lewy (CFL) criterion is used in FDS. This criterion is related to the convective terms of the governing equation. It is very important for the large-scale calculations where convective transport dominates diffusive. The estimated velocities are tested at each time step, δt, to ensure that the CFL condition is satisfied:

$$\delta t \max\left(\frac{|u_{ijk}|}{\delta x}, \frac{|v_{ijk}|}{\delta y}, \frac{|w_{ijk}|}{\delta z}\right) < 1 \tag{20}$$

The initial time step size is specified automatically in FDS by dividing the size of a mesh cell by the characteristic velocity of the flow. The default value of time step is:

$$\frac{5(\delta x \, \delta y \, \delta z)^{\frac{1}{3}}}{\sqrt{gH}} \tag{21}$$

During the calculation, the time step change and constrained by the convective and diffusive transport speeds by ensuring that the CFL condition is satisfied at each time step. The time step will eventually change into a quasi-stationary value when the fire environment will reach a quasi-steady state. The most critical point of a large eddy simulation is probably related to the size and the quality of calculation grid. This is a key parameter to be considered carefully at first since it plays a significant role in the precision of the FDS simulation results. With a grid size chosen carefully, LES gives reasonable results. Typically, tests of grid sensitivity must be carried out until we don't see significant differences in our results. Specifically, the determination of the grid size is important for the field near to an important gradient place as for example near the site of the fire. McGrattan *et al.* (2010b) have suggested that for simulations implying buoyant plumes, how a measure of the field flow is resolved, is given by the dimensionless expression $\frac{D^*}{\delta x}$ where D^* is a characteristic fire diameter given by

$$D^* = \left(\frac{Q}{\rho_0 C_p T_0 \sqrt{g}}\right)^{2/5} \tag{22}$$

McGrattan *et al.* (2010b) proved that a mesh size of about 0.1 of the characteristic fire diameter is acceptable to guarantee a reliable operation of FDS.

In this study, the physical model considered is a tunnel model of 12 m of length as shown in Fig. 1. The tunnel model is specified as a 1/20 scale of full scale tunnel. The cross section of tunnel is rectangular, with a different aspect ratio. The aspect ratio is defined as a tunnel height divided by its width. While maintaining the same cross-sectional area of tunnel, five different aspect ratios are considered in this study: A_r = 0.64 (tunnel A); 0.81 (tunnel B); 1.00 (tunnel C); 1.23 (tunnel D); 1.56 (tunnel E).

The tunnel model is made of "concrete". The

physical properties of this material (thermal conductivity, density and specific heat) are specified in the FDS model by the "MATL" command. The values used for the calculation are a thermal conductivity of 1.65 W/m.K, density of 2500 kg/m^3 and specific heat of 0.88 kJ/kg.K. The tunnel surfaces (walls, ceiling and floor) are thermally thick and smooth. The default velocity condition at the wall surface provided by FDS is assumed. The two surfaces of the tunnel extremities are both opened to the external ambient environment, but one (tunnel entry) is specified as an air flow inlet in the situation of longitudinal ventilation. The longitudinal ventilation velocity is set up by a supply air at ambient temperature introduced in the tunnel entry surface. The ambient temperature of the tunnel domain is prescribed via the TMPA parameter provided by FDS with values were about 20 °C in the series of tests simulations. The fire is simulated by a rectangular heat source having a section area of 8 cm × 10 cm. This source is placed in the center of the domain and in the middle of the two sidewalls, with its top surface is set at floor level. The heat release rate of the fire is changed into different values extend from 1.0 to 6.0 kW. The fire heat release rate is specified as a heat release rate per unit area applied to the source surface (command "HRRPUA" provided in FDS) and is treated as an average value. To produce smoke, a reaction type "Propane" was indicated with the soot yield is set equal to 0.1. A series of measuring stations placed at 1 cm below the ceiling of tunnel and at different heights above the floor is fixed in the FDS model to monitor the temperature and the CO concentration variation. The positions of the measuring points are shown in Fig. 2.
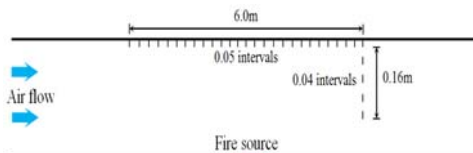
Fig. 2. Positions of the measuring points of temperature and CO concentration.

In this work, four different grid systems is chosen in order to test the grid size for tunnel C as shown in Table 1. The computation field is limited by the tunnel walls. The mesh is uniform in the transverse and vertical directions and it is refined in the longitudinal direction near to the heat source in the region covering the zone from 0.5 m upstream to 0.5 m downstream of the fire source. For our tests, temperature and velocity of the resulting flow predicted under the tunnel ceiling are selected as test parameters.

The distribution of temperature and velocity predicted under the tunnel ceiling with different grid systems are shown in Fig. 3. It can be seen that the results become slightly different with a finer mesh as tests no. 2-4. To limit the grid fineness and thus economize computation time, a total grid number of 500000 cells is finally used for tunnel C

with a distribution along the axes x, y and z is 400 × 50 × 25 cells.

Table 1 Grid system sensitivity study

Test no.	Grid number			Total cells	CPU time (hr)
	x	y	z		
1	300	50	25	375000	13,5
2	400	50	25	500000	19,58
3	440	50	25	550000	22.0
4	500	50	25	625000	28,17

When the tunnel geometry is modified, the grid will be increased or decreased consequently. It is made so that they have the same size in all cases. Finally, a grid system identified for each tunnel is finally used with a distribution along the axes *x*, *y* and *z* is shown in Table 2.
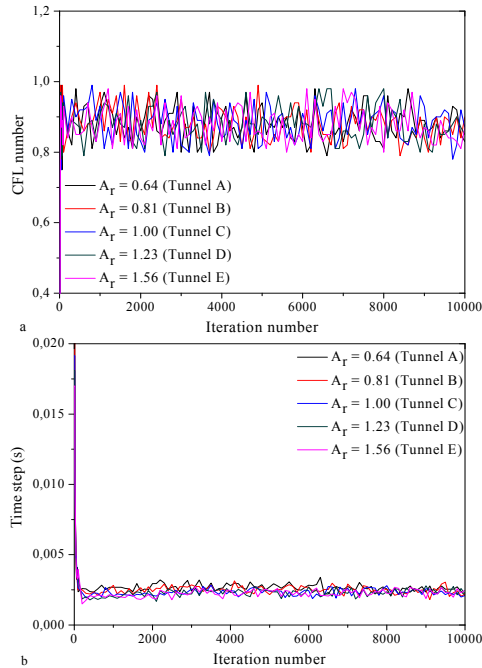
In Fig. 4, the CFL number and the time step for the different configurations studied are presented. The CFL condition which requires that the CFL number is less than or equal to 1 is satisfied with the CFL number varied generally in a range from 0.76 to 0.99 for all simulations. The simulation is performed up to 400 s. The time step size is adjusted by the solver itself. The time step in the simulations is in a range between 0.0022 and 0.02 s with an average value of around 0.0034 s.
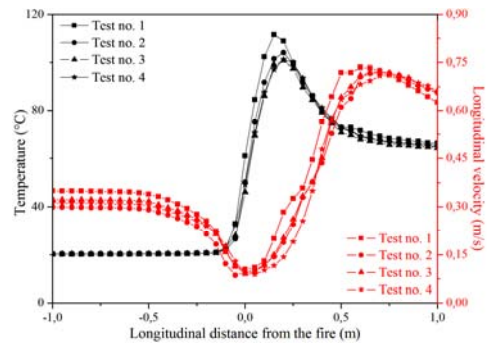

Fig. 3. Distribution of temperature and velocity predicted under the tunnel ceiling with different grid systems.

Table 2 Mesh size of FDS simulation

Tunnel	Mesh quantity			
	x	*y*	*z*	Total no. of meshes
A	400	64	20	512000
B	400	56	23	515200
C	400	50	25	500000
D	400	45	28	504000
E	400	40	32	512000

Fig. 4. CFL number and time step for FDS simulation for different studied configuration: a-CFL number, b-time step.
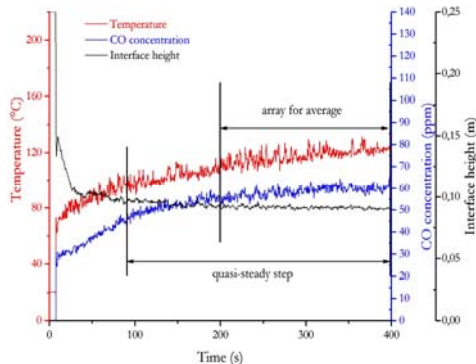
Fig. 5. Time evolution of the temperature, the CO concentration and the interface height under ceiling for 4.3 kW fire with ventilation velocity of 0.08 m/s for the tunnel C, 3 m downstream of the fire.

3. RESULTS AND DISCUSSION

3.1. Flow Parameters Analysis

Generally, at any position in the tunnel, the variables such as temperature, CO concentration and the smoke layer interface height undergo an apparent increase or a decrease in the first seconds after the fuel ignition until the plume flow generated by the fire reaches a relatively quasi-stationary stage where the quantities of these variables change slightly until the quasi-stationary step finished (by fuel exhaustion as example). Figure 5 shows the time evolution of the temperature, the CO concentration and the interface

height measured under ceiling at 3 m downstream from the 4.3 kW fire with 0.08 m/s ventilation velocity for the tunnel C. As shown in this figure, these variables reach a quasi-stationary step, and are slightly preserved to about 90 s. In this work, the interval between 200 s and the final time of the simulation is chosen to calculate the average of each variable studied.

3.2. Backlayering Length

The backlayering length can be determined by measuring the gas temperature under the tunnel ceiling. In effect, the temperature distribution of the smoke below the tunnel ceiling is marked a decrease at the end of the hot gas reverse flow, the presence of the backlayering can be easily detected and its length can be measured. An arrangement of measurement point placed at 1 cm below the tunnel ceiling is simulated in the FDS model to monitor the temperature variation. Figure 6 shows the temperature distribution measured for different longitudinal ventilation velocity for 6.0 kW fire for the tunnel with 1.0 aspect ratio. The backlayering length is determined until the first measuring station upstream of the heat source indicates the ambient temperature value (i.e. the temperature of measuring point nearest to fire is at ambient value). The critical value of the ventilation velocity is identified when the backlayering length tends towards zero. It can be clearly seen in Fig. 6 the decrease of backlayering length as the ventilation velocity increases. This is also shown in Fig. 7. This figure shows the backlayering length evolution as a function of the ventilation velocity for 6.0 kW fire for the tunnel C. Exponential approaching were tried to accord the decrease of backlayering length with the ventilation velocity. It can be seen that the backlayering length evolution as function of ventilation velocity fell into good exponential decay.
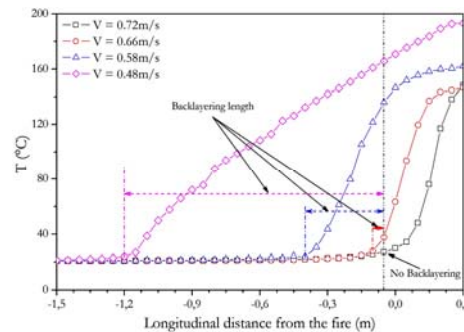

Fig. 6. Temperature distribution under ceiling with different longitudinal ventilation velocity for 6.0 kW fire for tunnel C.

3.3. Maximum Excess Temperature of Smoke Flow under Tunnel Ceiling

The maximum smoke temperature beneath the ceiling is an important parameter in designing and evaluating the building materials of tunnel. In Fig. 8 and Fig. 9, predictions of the maximum smoke temperature measured below the ceiling for all tests

of tunnels models are presented. It can be seen that the maximum smoke temperature increase as the aspect ratio decreased. The maximum smoke temperature provided by FDS are compared to those calculated by the model of Li *et al.* (2011) when the dimensionless ventilation velocity greater than 0.19. It can be seen that the present results agreed better with those obtained from model of Li *et al.* (2011). Furthermore, the maximum smoke temperature provided by FDS are compared to those given by the model of Kurioka *et al.* (2003). Also, the maximum smoke temperature predictions appeared to be in acceptable agreement with the measured value from Kurioka *et al.* (2003) model.
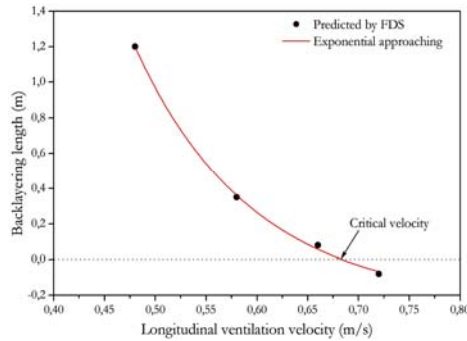
**Fig. 7. Backlayering length against ventilation velocity for 6.0 kW fire.**

3.4. CO Concentration Analysis

During a fire in tunnel, the majority of deaths are in relation primarily with the products released in smokes where an enormous quantity of toxic gases (for example CO) is generated because of an incomplete combustion. In this section, the effect of the aspect ratio of tunnel on the CO concentration will be studied. As illustration, the profiles of the CO concentration as a function of the longitudinal distance to the 4.3 kW fire with 0.08 m/s longitudinal ventilation velocity is presented in Fig. 10. It can be seen that the profiles are very similar in shape. The profiles show the high values of the CO concentration in the zone close to the heat source and as one move away from the fire, the profiles flatten and CO concentration undergoes a decrease in upstream and downstream of the heat source and it is maintained practically at an almost constant value along the tunnel length. Furthermore, it can be clearly seen from Fig. 10 that the CO concentration is sensitive to the aspect ratio variations. It can be observed a decrease in the CO concentration when the aspect ratio increases. This is probably due to the action of the buoyancy force which entrains an increase in the disruption of the smoke layer with fresh air having as a result more fresh air into the smoke layer and thus lowers the CO concentration that will be oxidized to CO_2. Indeed, during the development of the fire in the tunnel, the fluid particles and the resulting combustion products having a decreasing density with temperature, become lighter and begin to rise up toward the ceiling under the effect of the buoyancy force. They cause a significant

entrainment of ambient air by the flow smoke plume. At positions away from the heat source, the levels of CO decreases under a continuous dilution effect causing the oxidation of CO to CO_2.

3.5. Interface Height and Visibility

The estimate of the position of the interface between the upper layer, smoke-laden and the lower layer, fresh air-laden in a burning tunnel raises particular importance for fire protection and the evacuation of users. The descend of the smoke layer below the safety height (the safety height is a characteristic height of human eyes and it is equal to the 1.8 m above the ground in full scale (Yan *et al.* 2009)) provoke the loss of visibility that can be deadly to the users immediately, even at low concentration, in idle their displacement and thus the difficulty in to identify the emergency exits.
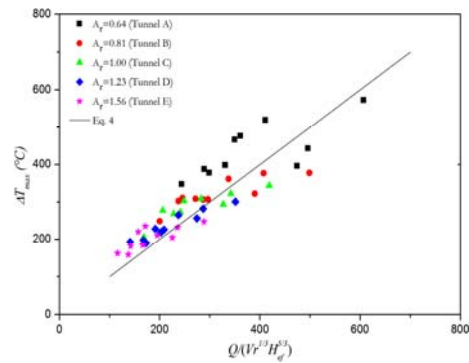
Fig. 8. Comparison of maximum smoke temperature predicted by FDS to those calculated by the model of Li *et al.* (2011) (V'>0.19).
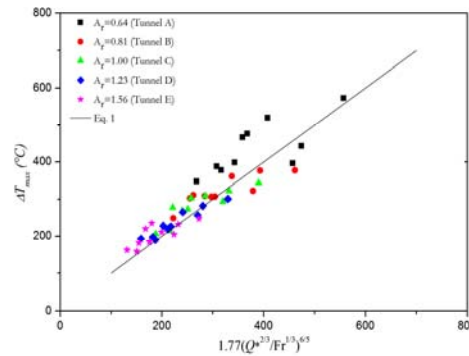

Fig. 9. Comparison of maximum smoke temperature predicted by FDS to those calculated by the model of Kurioka *et al.* (2003).

In FDS, a simple method for calculating the interface height, denoted h_{in}, is used considering a continuous temperature $T(z)$ as a function of the height z between the floor, $z = 0$, and ceiling, $z = H$ (McGrattan *et al.* 2010a). FDS assumed that the cooler lower layer temperature T_c is constant and equal to the temperature in the lowest mesh cell and the temperature of the hot layer, T_h, varies from the interface height by following a vertical thermal gradient. These two quantities are calculated by:

$$(H - h_{in})T_h + h_{in}T_c = \int_0^H T(z)dz = I_1 \quad (23)$$

$$(H - h_{in})\frac{1}{T_h} + h_{in}\frac{1}{T_c} = \int_0^H \frac{1}{T(z)}dz = I_2 \quad (24)$$
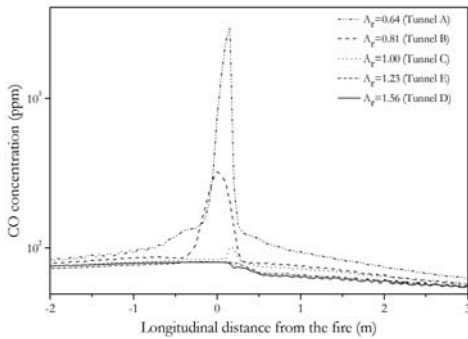
Fig. 10. Comparison of CO concentration under ceiling with aspect ratio for 4.3 kW fire with ventilation velocity of 0.08 m/s.

The interface height is determined, by resolving these two last quantities, by the following expression:

$$h_{in} = \frac{T_c(I_1 I_2 - H^2)}{I_1 + I_2 T_c^2 - 2T_c H} \quad (25)$$

As an illustration, the dimensionless interface height as a function of the distance to the 4.3 kW fire with 0.08 m/s longitudinal ventilation velocity for different aspect ratio is presented in Fig. 11. The dimensionless interface height is defined as interface height divided by tunnel height. It can be seen that the dimensionless interface height increases with the aspect ratio of the tunnel cross-section. This has as a result in sufficient influence on the visibility in the tunnel which will be a little lower.
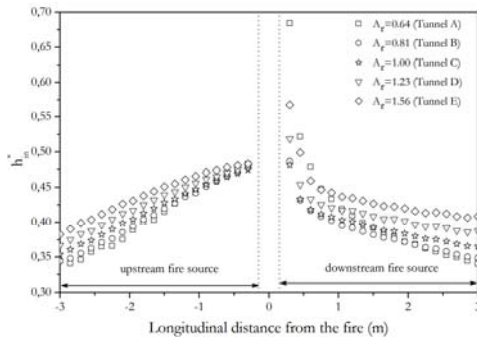
Fig. 11. Dimensionless interface height for 4.3 kW fire with ventilation velocity of 0.08 m/s for different aspect ratio.

The visibility regions less than 10 m with aspect ratio are shown in Fig. 12. It can deduce from this figure that the visibility regions less than 10 m are widening as the aspect ratio increases. Downstream of the heat source, it can be provided however a descent of the visibility region less than 10 m to the tunnel floor. The region of bad visibility near the floor is greater than the aspect ratio increases.
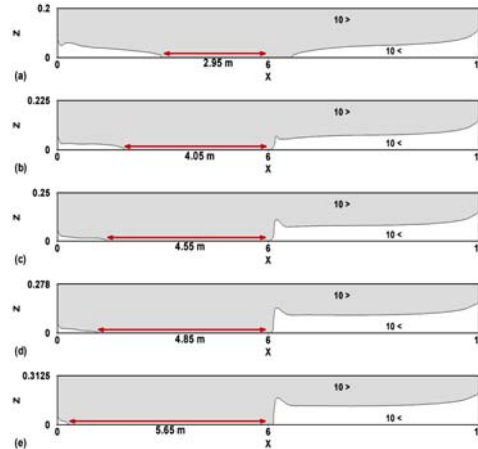
Fig. 12. Visibility region less than 10 m for 4.3 kW fire with ventilation velocity of 0.08 m/s for different aspect ratio: (a) $A_r = 0.64$, (b) $A_r = 0.81$, (c) $A_r = 1.00$, (d) $A_r = 1.23$, (e) $A_r = 1.56$.

4. CONCLUSION

In this study, CFD simulations using Fire Dynamic Simulator (FDS) were performed to analyze the smoke hazard in a longitudinally ventilated tunnel fires with different aspect. Comparison between the CFD predictions of maximum smoke temperature under the ceiling and the calculated values using the models of Li *et al.* (2011) and then of kurioka *et al.* (2003) show acceptable agreement. This study shows that the CO concentration reached their maximum value in the zone near to the heat source. Moving away from the fire, the CO concentration undergoes a decrease under the continuous dilution effect and is practically maintained at an almost constant value along the tunnel length. The tunnel cross-sectional geometry affects the CO production and an increase of aspect ratio correlates with a decrease in the CO concentration. Also, the results show that the CO concentration is negatively correlated with the longitudinal ventilation velocity. It can be suggested that the dimensionless interface height increases as the aspect ratio of tunnel cross-sectional increase which induced as well as a widening of the hot, smoke-laden layer.

REFERENCES

Gao, P. Z., S. L. Liu, W. K. Chow and N. K. Fong (2004). Large eddy simulations for studying tunnel smoke ventilation. *Tunn. Undergr. Sp. Technol. 19, 577–586.*

Hu, L. H., N. K. Fong, L. Z. Yang, W. K. Chow, Y. Z. Li and R. Huo (2007). Modeling fire-induced smoke spread and carbon monoxide transportation in a long channel: Fire Dynamics Simulator comparisons with measured data. *J. Hazard. Mater. 140, 293-298.*

Hu, L. H., W. Peng and R. Huo (2008). Critical wind velocity for arresting upwind gas and smoke dispersion induced by near-wall fire in a road tunnel. *J. Hazard. Mater. 150, 68-75.*

Kim, E., J. P. Woycheese and N. A. Dembsey (2008). Fire dynamics simulator (version 4.0) simulation for tunnel fire scenarios with forced, transient, longitudinal ventilation flows. *Fire Technol. 44, 137–166.*

Koylu, U. O. and G. M. Faeth (1991). Carbon monoxide and soot emissions from liquid-fueled buoyant turbulent diffusion flames", Combust. *Flame 87, 61–76.*

Kurioka, H., Y. Oka, H. Satoh and O. Sugawa (2003). Fire properties in near field of square fire source with longitudinal ventilation in tunnels, *Fire Saf. J. 38, 319-340.*

Li, Y. Z., B. Lei and H. Ingason (2011). The maximum temperature of buoyancy-driven smoke flow beneath the ceiling in tunnel fires. *Fire Saf. J. 46, 204-210.*

Massachusetts Highway Department and Bechtel/Parsons Brinckerhoff. (1995). *Memorial tunnel fire ventilation test program,* test report.

McGrattan, K., R. M. Dermott, S. Hostikka and J. Floyd (2010b). Fire Dynamics Simulator (Version 5): User's Guide. *NIST Special Publication 1019-5.*

McGrattan, K., S. Hostikka, J. Floyd, H. Baum, R. Rehm, W. Mell and R. McDermott (2010a). Fire Dynamics Simulator (Version 5): Technical Reference Guide. *NIST Special Publication 1018-5.*

PIARC (Technical Committee 5 Road Tunnels) (1999). *Fires and Smoke Control in Road Tunnels,* report 05.05.BEN.

Wang, H. Y. (2009). Prediction of soot and carbon monoxide production in a ventilated tunnel fire by using a computer simulation. *Fire Saf. J. 44, 394-406.*

Wen, J. X., K. Kang, T. Donchev and J. M. Karwatzki (2007). Validation of FDS for the prediction of medium-scale pool fires. *Fire Saf. J. 42, 127-138.*

Yan, T., S. MingHeng, G. YanFeng and H. JiaPeng (2009). Full-scale experimental study on smoke flow in natural ventilation road tunnel fires with shafts. *Tunn. Undergr. Sp. Technol. 24, 627–633.*

Zhang, J., X. Zhou, Q. Xu and L. Yang (2012). The inclination effect on CO generation and smoke movement in an inclined tunnel fire. *Tunn. Undergr. Sp. Technol. 29, 78-84.*

Zhang, W., A. Hamer, M. Klassen, D. Carpenter and R. Roby (2002). Turbulence Statistics in a Fire Room Model by Large Eddy Simulation, *Fire Saf. J. 37, 721-752.*